Biochimica et Biophysica Acta 1818 (2012) 651–657

Contents lists available at SciVerse ScienceDirect

Biochimica et Biophysica Acta

journal homepage: www.elsevier.com/locate/bbamem

The iron transporter ferroportin can also function as a manganese exporter

Michael S. Madejczyk *, Nazzareno Ballatori

Department of Environmental Medicine, University of Rochester School of Medicine, Rochester, NY 14642, USA

ARTICLE INFO

Article history:
Received 12 May 2011
Received in revised form 28 November 2011
Accepted 2 December 2011
Available online 8 December 2011

Keywords:
Ferroportin
FPN1
Manganese
Metal export
Divalent metal transporter
Xenopus laevis oocytes

ABSTRACT

The present study examined the hypothesis that the iron exporter ferroportin (FPN1/SLC40A1) can also mediate cellular export of the essential trace element manganese, using *Xenopus laevis* oocytes expressing human FPN1. When compared to oocytes expressing only the divalent metal transporter-1 (DMT1/NRAMP2), ^{54}Mn accumulation was lower in oocytes also expressing FPN1. FPN1-expressing oocytes exported more ^{54}Mn than control oocytes (26.6 ± 0.6% versus 7.1 ± 0.5%, respectively, over 4 h at pH 7.4 when preloaded with approximately 16 μM ^{54}Mn); however, there was no difference in ^{54}Mn uptake between control and FPN1-expressing oocytes. FPN1-mediated Mn export was concentration dependent and could be partially *cis*-inhibited by 100 μM Fe, Co, and Ni, but not by Rb. In addition, Mn export ability was significantly reduced when the extracellular pH was reduced from 7.4 to 5.5, and when Na^+ was substituted with K^+ in the incubation media. These results indicate that Mn is a substrate for FPN1, and that this export process is inhibited by a low extracellular pH and by incubation in a high K^+ medium, indicating the involvement of transmembrane ion gradients in FPN1-mediated transport.

1. Introduction

Manganese (Mn) is an essential trace element that is utilized in a number of important cellular processes; however, excess Mn can also be quite toxic [1]. Manganese neurotoxicity has been reported in occupationally exposed workers that have been chronically exposed to aerosols or dusts that contain high levels (>5 mg Mn/m^3) of manganese [2–4]. Under most conditions, Mn homeostasis is maintained in a large part via the actions of the intestine and liver: the intestine acts as an initial control of Mn levels by absorbing a variable amount of dietary Mn (1–5%), the main source of exposure [5], whereas hepatic biliary excretion serves as the major route of elimination for excess manganese [6]; although the specific transporters involved remain largely unknown.

In general, cellular manganese uptake appears to be mediated in part via similar mechanisms as iron [7–9]. This is not unexpected, as Mn and Fe share many similar physical and chemical properties. For example, these transition metals have similar atomic masses (54.94 and 55.85 amu, for Mn and Fe respectively), radii (127 pm for Mn versus 125 pm for Fe), and electron structure ([Ar] $4s^2$ $3d^5$ for Mn and [Ar] $4s^2$ $3d^6$ for Fe). Both elements have similar electronegativity (1.55 and 1.83) and ionization energies (717 and 763 kJ/mol for the 1st ionization), and exist in multiple oxidation states.

Indeed, Mn^{2+} is a known substrate for the divalent metal transporter-1 (Dmt1/Slc11A2/Nramp2), a highly conserved uptake transporter that utilizes the proton gradient to drive the uptake of a number of divalent metals, including Fe, Mn, Cd, Co, Cu, Zn, and to a lesser extent Ni and Pb [8,10]. The importance of Dmt1 in Fe and Mn homeostasis has been demonstrated utilizing the microcytic anemia mouse and the Belgrade (*b*) rat, which have a defect in Dmt1 transport activity and display reduced Fe and Mn uptake [11–13]. However, Dmt1 may not be essential for Mn transport, as suggested in a study by Crossgrove and Yokel [14] using *in situ* brain perfusion of *b*/*b*, +/*b*, and +/+ rats, which indicated the presence of other Mn transport mechanisms, although these have not yet been identified. Iron status can also influence Mn homeostasis. For example, iron deficiency is a risk factor for metal toxicity and an inverse relationship exists between dietary Fe and absorption and distribution of several other metals, including Mn [15–17]. Once taken up into cells, Mn can be sequestered in mitochondria [18], and possibly in other intracellular compartments, and can bind to many intracellular ligands.

The mechanisms of cellular Mn efflux are largely undefined, although given the overlap with Fe uptake transporters, it is possible that Mn and Fe may also share efflux transport mechanisms. Thus, one possibility is that Mn efflux is mediated by ferroportin (FPN1/SLC40A1), a major mediator of iron release [19]. Ferroportin was reported independently by three groups [20–22] and appears to transport iron in the ferrous form, although this has not been shown directly. To date, the energy source and the role of other ions

Abbreviations: DMT1, divalent metal transporter-1/NRAMP2; FPN1, ferroportin/SLC40A1

* Corresponding author at: Department of Biology, University of Rochester, 437 Hutchinson Hall, Box 270211, Rochester, NY 14627, USA. Tel.: +1 585 275 3877; fax: +1 585 275 2070.
E-mail address: Mike_Madejczyk@urmc.rochester.edu (M.S. Madejczyk).

0005-2736/$ – see front matter © 2011 Elsevier B.V. All rights reserved.
doi:10.1016/j.bbamem.2011.12.002

in FPN1-mediated transport have not been elucidated, and little information is available on FPN1's transport kinetics or substrate specificity [23]. This lack of this critical data can be explained in large part by the technical difficulties that are inherent in studying metal efflux transporters. First, efflux measurements require that the metal substrates somehow be loaded inside the cells or oocytes, and that they be loaded in the appropriate chemical form and concentration. This can be attempted by loading with a known plasma membrane uptake transporter, or by direct microinjection of the metal into the cell, but neither of these approaches will ensure that the metal will be in the appropriate chemical form, concentration, or localization within the cell. Second, once metals are delivered or taken up into cells, they can bind to many ligands and can be sequestered into various organelles, making it impossible to accurately assess intracellular concentrations of the transportable species, which are presumably the free divalent cations that are localized near the plasma membrane. Third, the exogenous radiolabeled metals will be diluted by unlabeled endogenous metals, further complicating the assessment of intracellular metal concentrations and chemical activities. Furthermore, the overexpression of FPN1 seems to be toxic to cells in culture, hampering the generation of stable cell lines [23]. Overall, these technical difficulties have made it, and will continue to make it extremely challenging to elucidate the kinetics and energetics of metal efflux from cells.

Interestingly, FPN1 is expressed in tissues involved in both iron and manganese homeostasis, including the developing and mature reticuloendothelial system, the duodenum, liver, and the pregnant uterus [20,24]. FPN1 has also been identified in cells of the central nervous system including those of the blood–brain barrier, choroids plexus, neurons, oligodendrocytes, astrocytes, and retina [25,26]. FPN1 is localized to the basolateral membrane of duodenal epithelial cells, and its overexpression in cultured cells results in intracellular iron depletion. Recently, Yin and colleagues [27] have implicated FPN1 as a potential Mn transporter. Using inducible HEK293T cell model, they showed that FPN1 expression reduced Mn-induced toxicity and decreased Mn accumulation. In addition, Mn was also able to increase FPN1 levels in native HEK cells and Fpn1 levels in mouse cerebellum and cortex. An increase in Fpn1 mRNA levels in response to Mn treatment was also seen by Troadec et al. [28].

To establish whether Mn is indeed a substrate for FPN1, and to gain insight into FPN1 mediated transport mechanism, the present study utilized *Xenopus laevis* oocytes injected with human *FPN1* cRNA. The results demonstrate that Mn is a substrate for FPN1, and thus suggest that this transporter may contribute to Mn homeostasis.

2. Materials and methods

2.1. Reagents

$^{54}MnCl_2$ (777.91 mCi/mg) and $^{55}FeCl_3$ (25.04 mCi/mg) were purchased from Perkin-Elmer Life and Analytical Sciences (Boston, MA). Other chemicals and reagents were obtained from Sigma-Aldrich Chemical Co. (St. Louis, MO) or J. T. Baker (Phillipsburg, NJ). Molecular biology reagents were purchased from Invitrogen (Carlsbad, CA); Clontech (Palo Alto, CA); Integrated DNA Technologies (Coralville, IA); Qiagen (Valencia, CA); Origene (Rockville, MD); Ambion (Austin, TX); and Promega (Madison, WI). Mature female *X. laevis* were purchased from Nasco (Fort Atkinson, WI). Animals were maintained under a constant light/dark cycle. Experiments were conducted in accordance with the guidelines of the NIH for care of laboratory animals.

2.2. Synthesis of cRNA

The full-length cDNA for human *DMT1A* was cloned from HepG2 cDNA, while *FPN1* cDNA was obtained from ATCC (Manassas, VA). Sequences were sub-cloned into the pSP64 poly A vector (Clontech, Mountain View, CA). Of the four isoforms of *DMT1*, *DMT1A + IRE* was chosen for these studies, as it demonstrates the most robust uptake of Fe when expressed in *Xenopus* oocytes [29]. A c-Myc epitope tag was added to the C-terminus of *FPN1*. End sequencing was performed at the University of Rochester Functional Genomics Center to verify clone identity and orientation. Capped cRNA was transcribed *in vitro* using SP6 mMESSAGE mMACHINE kit (Ambion, Austin, TX). cRNAs were precipitated with lithium chloride, resuspended in RNase-free water, and stored at −80 °C until used for oocyte microinjection.

2.3. Isolation and injection of Xenopus oocytes

Isolation of oocytes was performed as described by Goldin [30] and previously employed in our laboratory [31,32]. Frogs were anesthetized by immersion for 15–20 min in ice-cold 0.3% tricaine. Oocytes were removed from the ovary and washed with calcium-free OR-2 solution (82.5 mM NaCl, 2 mM KCl, 1 mM $MgCl_2$, and 5 mM HEPES–Tris; pH 7.5) and incubated at room temperature with gentle shaking for 80 min in OR-2 solution containing 1 mg/ml collagenase (type IA, Sigma). Oocytes were transferred to fresh collagenase solution after the first 40 min. Collagenase was removed by washing with OR-2 solution at room temperature. Defolliculated stage V and VI oocytes were selected and incubated at 18 °C in modified Barth's solution [88 mM NaCl, 1 mM KCl, 2.4 mM $NaHCO_3$, 0.82 mM $MgSO_4$, 0.33 mM Ca $(NO_3)_2$, 0.41 mM $CaCl_2$, and 20 mM HEPES–Tris (pH 7.4)]. After 30 min of incubation, oocytes were injected with 50 nl of *DMT1A* or *FPN1 cRNA* (10 ng each cRNA/oocyte), or a combination of both cRNAs (10 ng each cRNA/oocyte, 20 ng total cRNA), or sterile water. Glass micropipettes with a tip diameter of 20–40 μm were pulled on a Sutter Instrument model P80 pipette puller (Novato, CA). A Drummond (Broomall, PA) microinjector attached to a Brinkmann (Westbury, NY) MM33 micromanipulator was used for injection. Injected oocytes were cultured at 18 °C with a daily change of modified Barth's media containing gentamycin (0.05 mg/ml), sodium pyruvate (0.55 mg/ml), and theophylline (0.09 mg/ml). Oocytes with a homogeneous brown animal half and distinct equator line were selected for transport experiments after 3 days.

2.4. Uptake of ^{54}Mn

For uptake measurements, six to ten oocytes were incubated at 25 °C for 2 or 6 h with 400 μl of modified Barth's solution containing 1 or 500 μM $^{54}MnCl_2$ at pH 5.5 or 7.4, similar to those used by Yin and colleagues [27]. Uptake was stopped by transferring the oocytes to 2 ml of ice-cold modified Barth's solution containing 50 μM $MnCl_2$, and washed three times each with 2 ml of ice-cold modified Barth's solution. Two oocytes were placed in a polypropylene scintillation vial and were dissolved with 0.2 ml of 10% (w:v) SDS. Radioisotope was counted in a Beckman model 6500 scintillation counter (Fullerton, CA) after addition of 5 ml of Opti-Fluor (Packard Instruments, Downers Grove, IL). The Mn concentrations were selected based on previously measured Mn levels in mammalian blood and tissues [4,5], and based on intracellular levels in oocytes [this work].

2.5. Efflux of ^{54}Mn or ^{55}Fe

Healthy oocytes were injected with 50 nl of isotope solution (0.1 μCi/μl), containing various concentrations of $^{55}FeSO_4$ or $^{54}MnCl_2$ and inhibitors (see legends of Figs. 3–6 for individual composition). ^{55}Fe solutions contained 1 mM ascorbic acid to keep the Fe in a reduced state [22,23]. Intracellular concentration of substrates was calculated assuming an intracellular water space of 0.5 μl/oocyte for stage V and VI oocytes with a diameter of 1.0–1.3 mm [30]. After a 10–30-min pre-incubation at room temperature in modified Barth solution, oocytes were washed in 2.5 ml of modified Barth's solution to remove

extracellular radioisotopes and oocytes were transferred individually to polypropylene scintillation vials in 200 µl of modified Barth's solution (20 mM Hepes pH, 7.4; 20 mM Hepes pH 8.5; 20 mM MES pH 5.5; or 20 mM Hepes high K, where the NaCl was replaced by KCl, pH 7.4). In some experiments, 500 µM Mn or Fe was added to the media. Efflux was measured for 30 min or 4 h at 25 °C. At the end of the efflux period, the culture medium was removed and transferred to another scintillation vial, and the oocytes were dissolved in 0.2 ml of 10% SDS. Both the culture medium and oocytes were counted in a Beckman model 6500 scintillation counter (Fullerton, CA) after addition of 5 ml of Opti-Fluor (Packard Instruments, Downers Grove, IL). Efflux was expressed as the amount of radioactivity recovered in the culture medium divided by the total amount of radioactivity (i.e., the radioactivity in the culture medium plus that remaining in the oocytes).

2.6. Determination of endogenous oocyte Mn content by atomic absorption spectrometry

Oocyte manganese concentrations were determined using a Perkin-Elmer AAnalyst 600 atomic absorption spectrophotometer equipped with longitudinal Zeeman background correction and a transverse heated graphite furnace (Perkin-Elmer Life and Analytical Sciences, Shelton, CT). The matrix modifiers, palladium nitrate (5 µg) and magnesium nitrate (3 µg) were used to stabilize manganese during the pyrolysis furnace step. Argon was used to protect and purge the end capped graphite tubes with an internal flow of 250 ml/min. A Perkin-Elmer Lumina hollow cathode lamp was used. The spectrometer settings were: wavelength, 279.5 nm; slit width, 0.2 nm; Cu lamp current, 20 mA; background correction, Zeeman-effect; integration time, 4 s; injection volume, 15 µl; and matrix modifier volume, 5 µl. The AA600 furnace thermal program was: Dry1, 100°C, ramp time 1 s, hold time 20 s; Dry2, 150°C, ramp time 15 s, hold time 30 s; pyrolysis, 1300 °C, ramp time 10 s, hold time 20 s; atomization, 2000 °C, ramp time 0 s, hold time 4 s; clean out, 2450 °C, ramp time 1 s, hold time 3 s. Oocyte samples were wet ashed with ultra pure nitric acid (SeaStar Chemicals Inc., Sidney, BC, Canada). The residue was dissolved in a small volume of concentrated nitric acid and then diluted to 2% nitric acid with 18 mOhm deionized water prior to analysis.

2.7. Isolation of membrane-enriched oocyte fractions and protein analysis

The procedure for isolating membrane-enriched oocyte fractions was adapted from Geering et al. [33] and Cattori et al. [34]. Oocytes (100) were added to 2.5 ml ice-cold buffer containing 83 mM NaCl, 10 mM HEPES (*N*-2-hydroxyethylpiperazine-*N*′-2-ethanesulfonic acid; pH 7.4), 1 mM $MgCl_2$, 25 µl/ml protease inhibitor cocktail (Sigma P-8340), 1 mM phenylmethylsulfonyl fluoride, and 5 mM EDTA and homogenized with 20 strokes of a Dounce homogenizer (type A, loose-fitting pestle) immersed in ice. Samples were centrifuged twice at 1000 *g* at 4 °C for 10 min to remove yolk granules, and the resulting supernatant was centrifuged at 15,000 *g* at 4 °C for 1 h. The pellet (membrane-enriched fraction) was resuspended in 100 µl of buffer containing 10 mM Tris–HCl (pH 7.4), 50 mM NaCl, 50 mM NaF, 10 µl/ml protease inhibitor cocktail, 5 mM EDTA, 1 mM phenylmethylsulfonylfluoride and 1% Triton-X 100. The membrane-enriched fractions were stored at −20 °C until use. The protein concentration of each sample was determined using the *DC* Protein assay kit (Bio-Rad, Hercules, CA).

For immunoblot analysis of oocyte membrane-enriched fractions, samples were dissolved in Laemmli buffer (1:1, Bio-Rad), and SDS-PAGE was performed on 4–20% TGX Gels (Bio-Rad). For immunoblotting, proteins were electrophoretically transferred onto polyvinylidine fluoride membranes, blocked overnight with 5% nonfat milk in TBST [10 mM Tris–HCl (pH 8.0), 150 mM NaCl, and 0.05% (vol/vol) Tween-20] at 4 °C, and probed with the appropriate antibody in 5% nonfat milk in TBST for 2 h at room temperature. For detection of DMT1A, FPN1, and actin, primary antibodies against DMT1 (Sigma WH0004891M1), c-MYC (Sigma M4439), and actin (Sigma A2066), were each used at a dilution of 1:1000 (DMT1 and actin) or 1:500 (c-Myc). Blots were then probed with a peroxidase-linked secondary antibody, anti-mouse immunoglobulin G from rabbit (Sigma A9044) or anti-rabbit immunoglobulin G horseradish peroxidase-linked F $(ab)_2$ fragment from donkey (GE Healthcare, Buckinghamshire, UK), in 5% nonfat milk in TBST for 1 h at room temperature. Antibody binding was then detected using an enhanced chemiluminescence technique (Perkin-Elmer, Waltham, MA).

2.8. Statistical analysis

Data were analyzed by ANOVA, and the two-tailed Student's *t* test was used for comparisons with a control. $P<0.05$ was considered statistically significant. Data are expressed as means ± SEM of three or more independent experiments.

3. Results

To confirm the function of FPN1 in our model system, *Xenopus* oocytes that had been injected with cRNA for *FPN1-c-Myc* or H_2O as a control were subsequently microinjected with $^{55}FeSO_4$ to achieve intracellular concentrations of approximately 1 and 16 µM, and efflux was measured for 4 h at pH 7.4 (Fig. 1A). As expected [19–22], ^{55}Fe efflux was negligible in control oocytes, but was markedly enhanced in *FPN1*-injected oocytes (10.7 ± 0.3% and 8.9 ± 0.7% at 1 or 16 µM $^{55}FeSO_4$, respectively; Fig. 1A), indicating that functional FPN1 was being expressed in the oocytes.

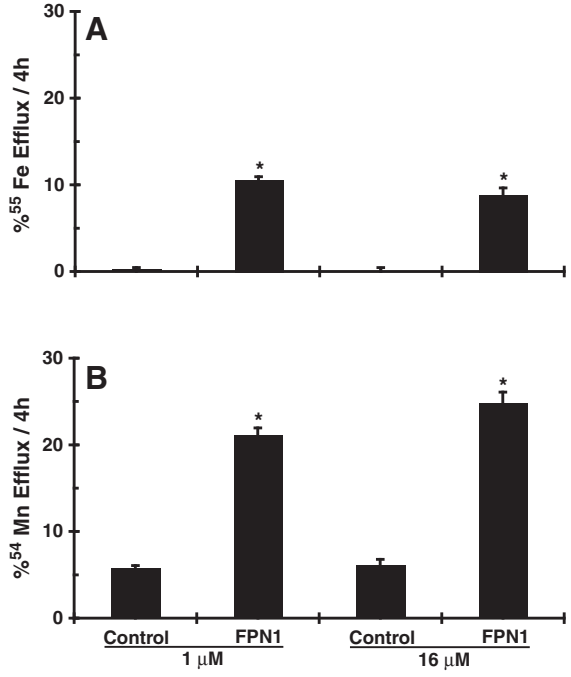

Fig. 1. FPN1-expressing oocytes demonstrate higher ^{55}Fe and ^{54}Mn efflux. Isolated *Xenopus* oocytes were injected with 10 ng *FPN1* cRNA or H_2O, and incubated for 3 days. Oocytes (6–10) were washed with modified Barth's solution (MB), and then injected with 50 nl of an 11 or 176 µM $^{55}FeSO_4$ (A) or $^{54}MnCl_2$ (B) solutions (final intracellular concentrations of approximately 1 and 16 µM), and allowed to recover for 10–30 min at room temperature. Oocytes were then placed individually in vials, 200 µl of fresh MB (pH 7.4) was added, and incubated for 4 h. The incubation media were removed and the oocytes lysed with 10% SDS. Both the media and oocyte were then counted. Data are presented as the mean of ^{55}Fe or ^{54}Mn released per oocyte in 4 h + SEM. *$p<0.05$ vs H_2O (control).

Interestingly, FPN1-expressing oocytes also demonstrated significant higher efflux of ^{54}Mn, suggesting that Mn is also a substrate for FPN1 (Fig. 1B). Note that whereas control oocytes released approximately 6% of the injected ^{54}Mn over a 4 h interval, FPN1-expressing oocytes released 20–25% of the ^{54}Mn over the same time period, when loaded with intracellular ^{54}Mn concentrations of 1 or 16 μM (Fig. 1B).

To test whether Mn is indeed a substrate of FPN1, additional studies were carried out in the *Xenopus* oocyte model. Oocytes were injected with cRNA for *FPN1-c-Myc*, *DMT1A*, a combination of *DMT1A* and *FPN1-c-Myc*, or H_2O as control, and uptake of ^{54}Mn for 2 or 6 h was evaluated in the presence of 1 or 500 μM $MnCl_2$ at pH 5.5, the optimal pH for DMT1A mediated uptake [8], or pH 7.4 (Fig. 2). At pH 7.4, ^{54}Mn uptake was negligible for all conditions tested with 1 μM $^{54}MnCl_2$ at both 2 and 6 h (Fig. 2A and C). At 2 h with 500 μM $^{54}MnCl_2$, accumulation was more pronounced compared to 1 μM Mn in all conditions, but still was not significantly greater than the endogenous uptake observed in water-injected oocytes (Fig. 2B). At 6 h, Mn accumulation was greater than control in the *DMT1A* injected and co-injected oocytes, most likely due to the ability of DMT1 to have some transport activity at pH 7.4 [35,36]; however, these data did not reach the threshold of significance (Fig. 2D).

As expected, ^{54}Mn uptake at pH 5.5 was robust in oocytes expressing DMT1A (Fig. 2E–H). In contrast, in FPN1-*c-Myc* expressing oocytes ^{54}Mn uptake was similar to controls (Fig. 2E–H). When exposed to 1 μM Mn for 2 h, ^{54}Mn accumulation was nearly identical between DMT1A alone and DMT1A + FPN1-*c-Myc* (8.4 ± 0.5 and 8.7 ± 1.3 pmol/oocyte, respectively; Fig. 2E). Interestingly, at 6 h the co-expression of FPN1 led to lower ^{54}Mn accumulation versus DMT1A alone (14.9 ± 1.2 versus 9.8 ± 0.6 pmol/oocyte). When exposed to 500 μM Mn (Fig. 2F and H), ^{54}Mn accumulation was higher in DMT1A expressing oocytes in both concentration and time dependent manners. As seen at the 6 h time point with 1 μM Mn, co-expression of FPN1 led to lower ^{54}Mn accumulation at both 2 and 6 h (135 ± 35 versus 58 ± 15 and 230 ± 14 versus 141 ± 10 pmol/

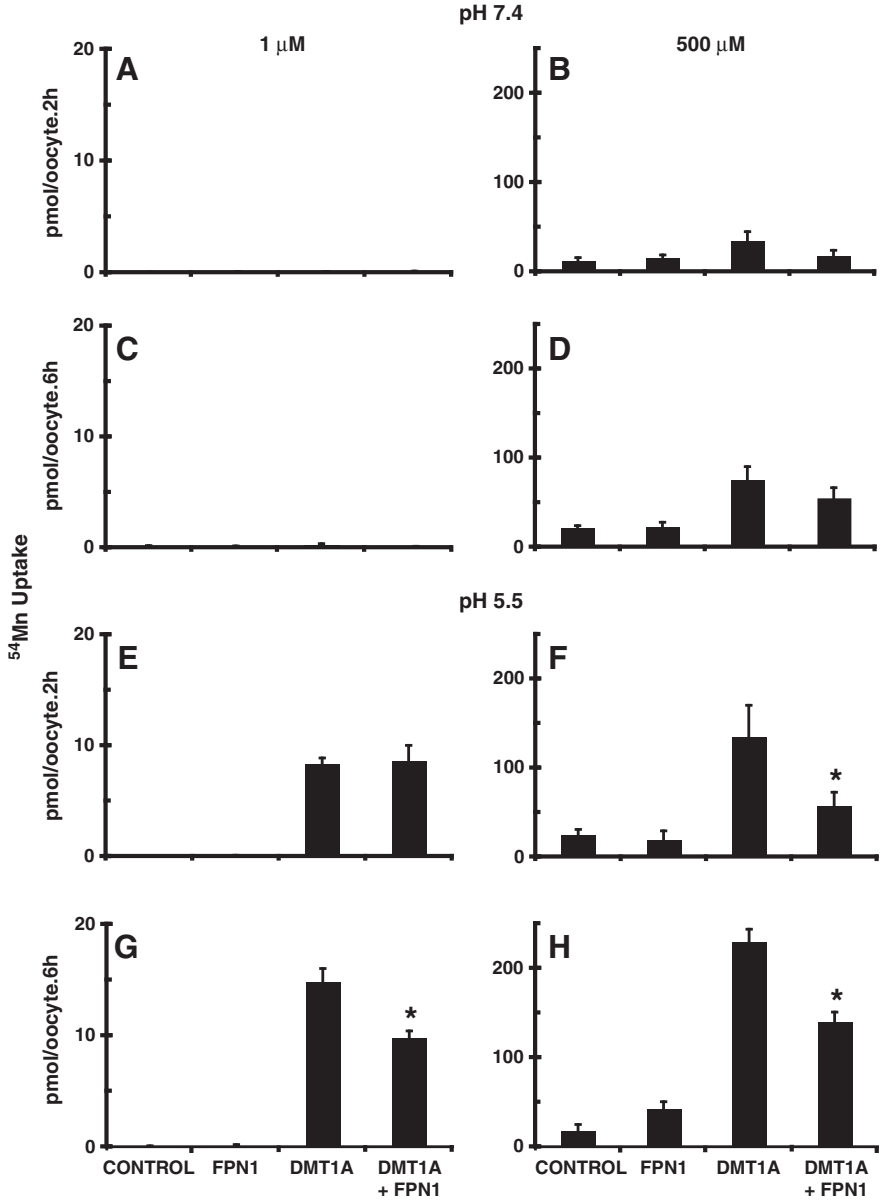

Fig. 2. FPN1 co-expression can decrease DMT1A-mediated accumulation of ^{54}Mn in a time and concentration-dependent manner. Isolated *Xenopus* oocytes were injected with 10 ng of cRNA for *FPN1*, *DMT1A*, both *FPN1* and *DMT1*, or H_2O and incubated for 3 days. Oocytes (4–10) were washed with modified Barth's solution (MB), and then incubated in fresh MB containing 1 μM (A, C, E, G) or 500 μM (B, D, F, H) $^{54}MnCl_2$ at 25 °C for 2 h (A, B, E, F) or 6 h (C, D, G, H) at pH 7.4 (A–D) or 5.5 (E–H). Oocytes were then washed three times in ice-cold MB containing 50 μM cold $MnCl_2$, lysed with 10% SDS and counted. Data are presented as the mean ^{54}Mn per oocyte + SEM. *$p<0.05$ vs DMT1A.

oocyte, respectively). These accumulation results suggest either that DMT1-mediated uptake activity was diminished, or that FPN1 may be acting as a Mn efflux transporter. The observations also suggest that this Mn efflux mechanism is both time and concentration dependent. In contrast, no significant difference in ^{54}Mn accumulation was observed between control oocytes and oocytes expressing FPN1 at any pH, time, or concentration tested, indicating that FPN1 is not able to function as a Mn uptake transporter.

Western blots were performed to verify expression of DMT1A and FPN1-c-Myc. Plasma membrane-enriched fractions were subject to SDS-PAGE, and probed with either anti-DMT1 or anti-c-Myc antibodies for detecting the FPN1-c-Myc polypeptide. DMT1 protein was detected as multiple bands in *DMT1A* and *DMT1A + FPN1* injected oocytes, but was absent in control and *FPN1* injected oocytes (Fig. 3A). The major band was around 55 kDa, while staining was also seen from approximately 60–100 kDa. These results are consistent with those seen by Tabuchi et al. [37], who examined the expression of DMT1 isoforms in multiple cell lines. FPN1 was detected in FPN1 and DMT1A + FNP1 injected oocytes as a band of 62–70 kDa, consistent with results seen by McKie et al. [22], but was absent in control and *DMT1A* injected oocytes (Fig. 3B). Note that DMT1A and FPN1 expression levels appeared to be slightly lower in oocytes co-expressing these proteins when compared to those expressing the individual transporters, possibly due to competition of the injected exogenous cRNAs for translation machinery. The apparent reduced DMT1 expression may have contributed to the diminished Mn accumulation noted in Fig. 2.

Thus, to test whether the lower Mn accumulation seen in oocytes co-expressing DMT1A and FPN1 was actually due to the efflux of Mn by FPN1, additional studies examined the ability of FPN1 to directly export ^{54}Mn. Control and FPN1 expressing oocytes were microinjected with increasing intracellular $^{54}MnCl_2$ concentrations, and efflux was measured for 4 h at pH 7.4 (Fig. 4). FPN1 expressing oocytes released more ^{54}Mn at each concentration tested, and the amount released was concentration dependent. When corrected for the endogenous ^{54}Mn efflux, the calculated FPN1-mediated efflux was non-linear and suggested saturability (Fig. 4); however, for the reasons noted in the Introduction section, these data are unsuitable for calculating kinetic parameters.

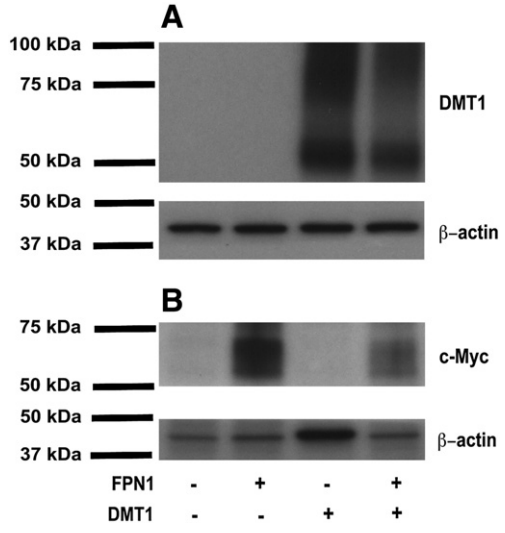

Fig. 3. Western blot analysis of *Xenopus* oocytes expressing human DMT1 and FPN1-c-Myc. *Xenopus* oocytes were injected with 10 ng of cRNA for *FPN1*, *DMT1A*, both *FPN1* and *DMT1*, or H_2O and incubated for 3 days. For immunoblot detection, membrane-enriched fractions were subject to SDS-PAGE. Blots were probed with primary antibodies against DMT1, c-Myc, and actin, and detected with horseradish peroxidase-linked secondary antibodies. For DMT1 analysis (A), 10 μg of protein was used in each lane, and for FPN1 analysis 40 μg was used (B).

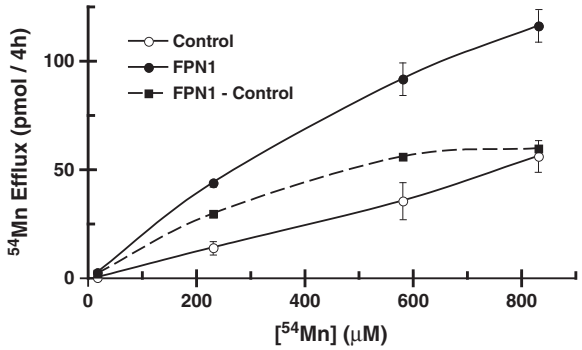

Fig. 4. FPN1-expressing oocytes have higher ^{54}Mn efflux, and efflux is concentration dependent. Isolated *Xenopus* oocytes were injected with 10 ng *FPN1* cRNA or H_2O, and incubated for 3 days. Oocytes (6–10) were washed with modified Barth's solution (MB), and then injected with 50 nl of $^{54}MnCl_2$ solutions to achieve final intracellular concentrations ranging from 16 to 830 μM, and allowed to recover for 10–30 min at room temperature. Oocytes were then individually placed in vials, 200 μl of fresh MB (pH 7.4) was added, and incubated for 4 h. The incubation media was removed and the oocytes lysed with 10% SDS. Both the media and oocyte were then counted. Data are presented as the mean of ^{54}Mn released per oocyte in 4 h + SEM. *$p<0.05$ vs H_2O (control). FPN1-mediated efflux (dotted line) was calculated by subtracting the control values from FPN1 values.

Analysis of endogenous Mn levels in oocytes using atomic absorption spectroscopy revealed levels of 86 ± 3 pmol/oocyte, or an approximate intracellular concentration of 173 ± 6 μM assuming an intracellular water volume of 0.5 μl/oocyte; however, this technique only allowed for the determination of total Mn and not free Mn^{2+}. Because Mn can be sequestered into intracellular organelles such as the mitochondria [18], the injected concentrations provide only estimates of total Mn concentrations.

To examine the specificity of ^{54}Mn efflux via FPN1, other metals were co-injected with the $^{54}MnCl_2$ (Fig. 5). Competing metals were injected to an estimated intracellular concentration of 100 μM, while $^{54}MnCl_2$ was injected to 16 μM. Higher concentrations of metals were not used in order to avoid toxicity to the oocytes. Even at this low $M^{(2)+}$ to Mn ratio (approximately 6:1), Fe^{2+}, Co^{2+}, and Ni^{2+} were all able to significantly *cis*-inhibit ^{54}Mn efflux via FPN1, whereas Zn^{2+}, Pb^{2+}, Cd^{2+}, and the monovalent Rb^{+} had no effect, suggesting that FPN1 may be able to transport different divalent metals with differing affinities.

To gain insight into the potential driving force for transport on FPN1, efflux was compared at pH values of 5.5, 7.4, and 8.5 (Fig. 6A). At all three pH values, FPN1 mediated ^{54}Mn efflux was

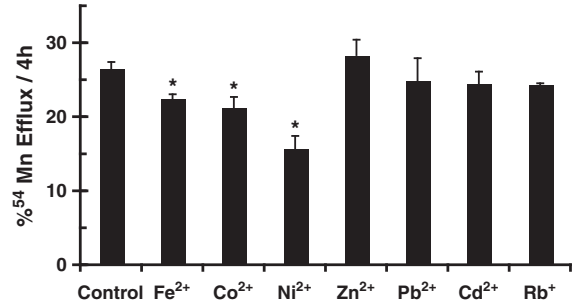

Fig. 5. FPN1-mediated ^{54}Mn efflux is *cis*-inhibited by Fe, Co, and Ni. Isolated *Xenopus* oocytes were injected with 10 ng *FPN1* cRNA or H_2O, and incubated for 3 days. Oocytes (6–10) were washed with modified Barth's solution (MB), and then injected with 50 nl of a 176 μM $^{54}MnCl_2$ solution alone or co-injected with 1.1 mM of the indicated metals (final intracellular concentration of approximately 16 μM for ^{54}Mn and 100 μM for the other metals) and allowed to recover for 10–30 min at room temperature. Oocytes were then individually placed in vials, 200 μl of fresh MB (pH 7.4) was added, and incubated for 4 h. The incubation media were removed and the oocytes lysed with 10% SDS. Both the media and oocyte were then counted. Data are presented as the mean of ^{54}Mn released per oocyte in 4 h + SEM. *$p<0.05$ vs control.

significantly greater than in control oocytes. Interestingly, at pH 5.5, but not 8.5, Mn efflux was significantly lower than at pH 7.4. This indicates the potential role for an outward proton gradient as a driving force for Mn efflux via FPN1. In addition, efflux was examined in a high K^+ media to depolarize the cell membrane potential (Fig. 6B). In the high K^+ media, FPN1 mediated Mn efflux was about one-third lower (18.8 ± 1.2% versus 26.6 ± 0.6% efflux in 4 h, respectively), indicating that the membrane potential or the Na^+ or K^+ gradients may also influence FPN1-mediated Mn export.

To further explore the mechanism of transport, *trans*-stimulation experiments were performed in which ^{54}Mn efflux was measured in media containing 500 μM Fe, Ni, or unlabeled Mn (Fig. 7). However, these metals were unable to stimulate ^{54}Mn efflux, and in fact actually inhibited efflux, with Ni being able to fully inhibit ^{54}Mn efflux (Fig. 7), indicating *trans*-inhibition of efflux. The mechanism for this *trans*-inhibition is as yet undefined, but it provides additional evidence that Mn is a substrate for FPN1.

4. Discussion

The present results provide direct evidence that Mn is a substrate for FPN1, and provide clues as to FPN1's transport mechanism. In particular, FPN1 mediated transport appears to be unidirectional, and is inhibited at low pH and by the substitution of Na^+ with K^+ in the culture medium. This putative role of FPN1 in Mn export is consistent with its cellular and subcellular localization. FPN1 is expressed in tissues involved in both Fe and Mn homeostasis, including the developing and mature reticuloendothelial system, the duodenum, liver, and

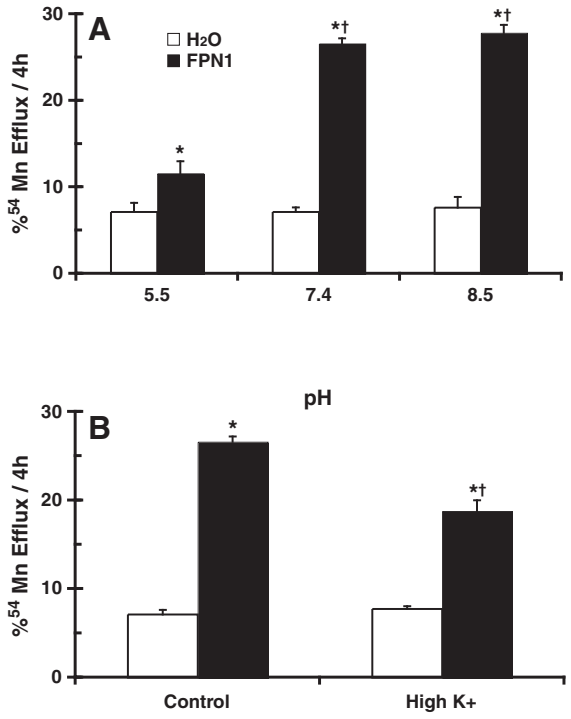

Fig. 6. FPN1 mediated ^{54}Mn efflux is inhibited in medium of low pH, or in which the Na^+ is substituted with K^+. Isolated *Xenopus* oocytes were injected with 10 ng *FPN1* cRNA or H_2O, and incubated for 3 days. Oocytes (6–10) were washed with modified Barth's solution (MB), and then injected with 50 nl of a 176 μM $^{54}MnCl_2$ solution (final intracellular concentration of approximately 16 μM) and allowed to recover for 10–30 min at room temperature. Oocytes were then individually placed in vials containing either: A. 200 μl of fresh MB (pH 5.5, 7.4, or 8.5), or B. 200 μl of fresh MB (pH 7.4) or high K^+ MB, and incubated for 4 h. The incubation media were removed and the oocytes lysed with 10% SDS. Both the media and oocyte were then counted. Data are presented as the mean percent of ^{54}Mn released per oocyte in 4 h + SEM. *p<0.05 vs H_2O (control), †p<0.05 vs FPN1 at either pH 5.5 (panel A), or vs FPN1 in control media (panel B).

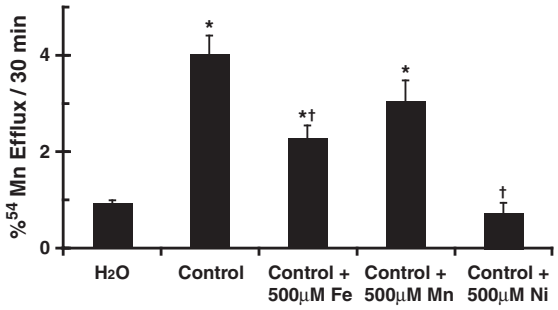

Fig. 7. FPN1-mediated ^{54}Mn efflux is *trans*-inhibited by extracellular Fe and Ni. Isolated *Xenopus* oocytes were injected with 10 ng *FPN1* cRNA or H_2O, and incubated for 3 days. Oocytes (6–10) were washed with modified Barth's solution (MB), and then injected with 50 nl of a 176 μM $^{54}MnCl_2$ solution (final intracellular concentration of approximately 16 μM) and allowed to recover for 10–30 min at room temperature. Oocytes were then individually placed in vials, 200 μl of fresh MB (pH 7.4) alone or with 500 μM Fe, Mn, or Ni was added, and incubated for 30 min. The incubation media were removed and the oocytes lysed with 10% SDS. Both the media and oocyte were then counted. Data are presented as the mean percent of ^{54}Mn released per oocyte in 4 h or 30 min + SEM. *p<0.05 vs H_2O, †p<0.05 vs control.

the pregnant uterus [20,24], as well as cells of the central nervous system, including those of the blood–brain barrier, choroids plexus, neurons, oligodendrocytes, astrocytes, and retina [25,26]. FPN1 is localized to the basolateral membrane of the duodenal epithelial cells, where it acts in concert with DMT1 to mediate the *trans*-cellular movement of Fe, and possibly Mn, from the intestinal lumen into the blood. Mutations in FPN1 lead to a form of hemochromatosis known as "ferroportin disease," which is characterized by a progressive iron accumulation in organs, predominantly in reticuloendothelial macrophages [38], while deletion is embryonically lethal [19].

The present results demonstrate that oocytes expressing FPN1 are able to release nearly four-fold as much ^{54}Mn as control oocytes (Fig. 1). Further analysis demonstrated that the efflux was concentration dependent (Fig. 4), and appeared to be saturable, but kinetic parameters could not be calculated for this export mechanism for the reasons described in the Introduction section. Additional evidence that Mn is indeed a substrate for FPN1 comes from the finding that Mn efflux could be *cis*-inhibited by divalent Fe, Co, and Ni. Even though the excess of injected metals was modest (approximately 6:1), there was a 15–40% inhibition of Mn efflux, with Ni having the greatest effect (Fig. 5). It is not surprising that these other metals may also be substrates for FPN1, as they are similar both structurally and chemically. The *Arabadopsis* orthologues of human FPN1 appear to be involved in both Fe and Co homeostasis [39], also indicating a broad metal substrate specificity for this FPN1 orthologue. Taken together, these data provide strong evidence that Mn is indeed a substrate for FPN1.

Insight into the mechanism of FPN1-mediated transport was obtained by examining whether extracellular pH had an effect on efflux. FPN1-mediated Mn efflux was robust and similar between pH 7.4 and 8.5; however, it was significantly decreased at pH 5.5, suggesting that the H^+ gradient from in to out may be a part of the driving force for efflux. In addition to the proton gradient, other ion gradients may also play a role. Incubation in high K^+ media resulted in a decrease in Mn efflux, indicating that Mn efflux via FPN1 may be dependent on the membrane potential or on the Na^+ or K^+ gradients.

In contrast to the ability of FPN1 to mediate Mn export, this protein had no effect on Mn uptake in cells incubated with either 1 or 500 μM Mn, at pH 5.5 or 7.4 (Fig. 2). This indicates that transport via FPN1 is unidirectional, and is supported by the results of McKie et al., [22] who reported no Fe uptake via FPN1 when expressed in *Xenopus* oocytes. Interestingly, Ni was able to *cis*-inhibit (Fig. 5) and *trans*-inhibit (Fig. 7) Mn efflux. The reason for this is unknown, but one possible explanation is that Ni may bind with high affinity to both the inward- and outward-facing conformations of FPN1, thus

inhibiting export from both the intracellular and extracellular faces of the protein.

In summary, the present study provides direct evidence that Mn is a substrate for FPN1, and suggests that FPN1 may be a multi-specific metal efflux carrier. Transport via FPN1 is reduced by both low pH and by substituting K^+ for Na^+ in the culture medium, suggesting that transmembrane ion or electrical gradients influence transport activity; however, additional research is needed to further characterize the substrate specificity and driving force for FPN1. Although both Fe and Mn appear to be well transported in this model system (Fig. 1), due to the challenges to studying efflux mentioned earlier, it is difficult to speculate on their relative affinities for the transporter. The conclusion that Mn and Fe share a mechanism for efflux provides additional insight into the interplay between iron and manganese absorption and toxicity, and suggests that FPN1 may be a target for modifying cellular levels of these metals. It is well established that iron deficiency is a risk factor for increased manganese absorption in the gut (Heilig et al., for a review [40]), and DMT1 mRNA levels are dramatically upregulated in enterocytes of iron-deficient rats [8]. As Mn levels rise in the cell, FPN1 may be up regulated in response [27,28], and this enhanced FPN1 expression could stimulate Mn absorption into the bloodstream. Additional studies are needed to test this model, and to establish the physiological relevance of FPN1 to Mn absorption.

Acknowledgements

We thank Robert Gelein for assistance with the atomic absorption spectrometry, and Dr. Christine Hammond for assistance with some of the experiments. This work was supported in part by the National Institutes of Health/National Institute of Environmental Health Sciences [Grants ES01247, ES07026]; and the National Institutes of Health/National Institute of Diabetes and Digestive and Kidney Diseases [Grant DK067214].

References

[1] J.S. Crossgrove, W. Zheng, Manganese toxicity upon overexposure, NMR Biomed. 17 (2004) 544–553.
[2] D. Mergler, G. Huel, R. Bowler, A. Iregren, S. Belanger, M. Baldwin, R. Tardif, A. Smargiassi, L. Martin, Nervous system dysfunction among workers with long-term exposure to manganese, Environ. Res. 64 (1994) 151–180.
[3] P.K. Pal, A. Sami, D.B. Calne, Manganese neurotoxicity: a review of clinical features, imaging, and pathology, Neurotoxicology 20 (1999) 227–238.
[4] Agency for Toxic Substance and Disease Registry (ATSDR), Toxicological Profile for Manganese, US Department of Health and Human Services, Public Health Service, Atlanta, GA, 2008.
[5] J.L. Aschner, M. Aschner, Nutritional aspects of manganese homeostasis, Mol. Aspects Med. 26 (2005) 353–362.
[6] P.S. Papavasilou, S.T. Miller, G.C. Cotzias, Role of liver in regulating distribution and excretion of manganese, Am. J. Physiol. 211 (1966) 211–216.
[7] M. Aschner, M. Gannon, Manganese (Mn) transport across the rat blood–brain barrier: saturable and transferrin-dependent transport mechanisms, Brain Res. Bull. 33 (1994) 345–349.
[8] H. Gunshin, B. Mackenzie, U.V. Berger, Y. Gunshin, M.F. Romero, W.F. Boron, S. Nussberger, J.L. Gollan, M.A. Hediger, Cloning and characterization of a mammalian proton-coupled metal-ion transporter, Nature 388 (1997) 482–488.
[9] E.A. Malecki, B.M. Cook, A.G. Devenyi, J.L. Beard, J.R. Connor, Transferrin is required for normal distribution of 59Fe and 54Mn in mouse brain, J. Neurol. Sci. 170 (1999) 112–118.
[10] M.D. Garrick, S.T. Singleton, F. Vargas, H.C. Kuo, M. Knopfel, T. Davidson, M. Costa, P. Paradkar, J.A. Roth, L.M. Garrick, DMT1: which metals does it transport? Biol. Res. 39 (2003) 79–85.
[11] A.C. Chua, E.H. Morgan, Manganese metabolism is impaired in the Belgrade laboratory rat, J. Comp. Physiol. 167 (1997) 361–369.
[12] M.D. Fleming, C.C. Trenor, M.A. Su, D. Foernzler, D.R. Beier, W.F. Dietrich, N.C. Andrews, Microcytic anaemia mice have a mutation in Nramp2, a candidate iron transporter gene, Nat. Genet. 16 (1997) 383–386.
[13] M.D. Fleming, M.A. Romano, M.A. Su, L.M. Garrick, M.D. Garrick, N.C. Andrews, Nramp2 is mutated in the anemic Belgrade (b) rat: evidence of a role for Nramp2 in endosomal iron transport, Proc. Natl. Acad. Sci. U. S. A. 95 (1998) 1148–1153.
[14] J.S. Crossgrove, R.A. Yokel, Manganese distribution across the blood–brain barrier III. The divalent metal transporter-1 is not the major mechanism mediating brain manganese uptake, Neurotoxicology 25 (2004) 451–460.
[15] K. Erikson, Z.K. Shihabi, J. Aschner, M. Aschner, Manganese accumulates in iron-deficient rat brain regions in a heterogeneous fashion and is associated with neurochemical alterations, Biol. Trace Elem. Res. 87 (2002) 143–156.
[16] K.M. Erikson, T. Syversen, E. Steinnes, M. Aschner, Globus pallidus: a target brain region for divalent metal accumulation associated with dietary iron deficiency, J. Nutr. Biochem. 15 (2004) 335–341.
[17] S.J. Garcia, K. Gellein, T. Syversen, M. Aschner, Iron deficient and manganese supplemented diets alter metals and transporters in the developing rat brain, Toxicol. Sci. 95 (2007) 205–214.
[18] C.E. Gavin, K.K. Gunter, T.E. Gunter, Manganese and calcium transport in mitochondria: implications for manganese toxicity, Neurotoxicology 20 (1999) 445–454.
[19] A. Donovan, C.A. Lima, J.L. Pinkus, G.S. Pinkus, L.I. Zon, S. Robine, N.C. Andrews, The iron exporter ferroportin/Sc40a1 is essential for iron homeostasis, Cell Metab. 1 (2005) 191–200.
[20] S. Abboud, D.J. Haile, A novel mammalian iron-regulated protein involved in intracellular iron metabolism, J. Biol. Chem. 275 (2000) 19906–19912.
[21] A. Donovan, A. Brownlie, Y. Zhou, J. Shepard, S.J. Pratt, J. Moynihan, B.H. Paw, A. Drejer, B. Barut, A. Zapata, T.C. Law, C. Brugnara, S.E. Lux, G.S. Pinkus, J.L. Pinkus, P.D. Kingsley, J. Palis, M.D. Fleming, N.C. Andrews, L.I. Zon, Positional cloning of zebrafish ferroportin 1 identifies a conserved vertebrate iron exporter, Nature 403 (2000) 776–781.
[22] A.T. McKie, P. Marciani, A. Rolfs, K. Brennan, K. Wehr, D. Barrow, S. Miret, A. Bomford, T.J. Peters, F. Farzaneh, M.A. Hediger, M.W. Hentze, R.J. Simpson, A novel duodenal iron-regulated transporter, IREG1, implicated in the basolateral transfer of iron to the circulation, Mol. Cell 5 (2000) 299–309.
[23] A.T. McKie, D.J. Barlow, The SLC40 basolateral iron transporter family (IREG1/ferroportin/MTP1), Pflugers Arch. 447 (2004) 801–806.
[24] A.S. Zhang, S. Xiong, H. Tsukamoto, C.A. Enns, Localization of iron metabolism-related mRNAs in the rat liver indicate that HFE is expressed predominantly in hepatocytes, Blood 103 (2004) 1509–1514.
[25] P. Hahn, T. Dentchev, Y. Qian, T. Rouault, Z.L. Harris, J.L. Dunaief, Immunolocalization and regulation of iron handling proteins ferritin and ferroportin in the retina, Mol. Vis. 10 (2004) 598–607.
[26] L.J. Wu, A.G. Leenders, S. Cooperman, E. Meyron-Holtz, S. Smith, W. Land, R.Y. Tsai, U.V. Berger, Z.H. Sheng, T.A. Rouault, Expression of the iron transporter ferroportin in synaptic vesicles and the blood–brain barrier, Brain Res. 1001 (2004) 108–117.
[27] Z. Yin, H. Jiang, E.Y. Lee, M. Ni, K.M. Erickson, D. Milatovic, A.B. Bowman, M. Aschner, Ferroportin is a manganese-responsive protein that decreases manganese cytotoxicity and accumulation, Neurochemistry 112 (2010) 1190–1198.
[28] M.B. Troadec, D.M. Ward, E. Lo, J. Kaplan, I. De Domenico, Induction of FPN1 transcription by MTF-1 reveals a role for ferroportin in transition metal efflux, Blood 116 (2010) 4657–4664.
[29] B. Mackenzie, H. Takanaga, N. Hubert, A. Rolfs, M.A. Hediger, Functional properties of multiple isoforms of human divalent metal-ion transporter 1 (DMT1), Biochem. J. 403 (2007) 59–69.
[30] A.L. Goldin, Maintenance of *Xenopus laevis* and oocyte injection, Methods Enzymol. 207 (1992) 266–279.
[31] N. Ballatori, W. Wang, L. Li, A.T. Truong, An endogenous ATP-sensitive glutathione *S*-conjugate efflux mechanism in *Xenopus laevis* oocytes, Am. J. Physiol. 270 (1996) R1156–R1162.
[32] N. Ballatori, W.V. Christian, J.Y. Lee, P.A. Dawson, C.J. Soroka, J.L. Boyer, M.S. Madejczyk, N. Li, OSTα-OSTβ, a major basolateral bile acid and steroid transporter in human intestinal, renal, and biliary epithelia, Hepatology 42 (2005) 1270–1279.
[33] K. Geering, I. Theulaz, F. Verrey, M.T. Hauptle, B.C. Rossier, A role for the -subunit in the expression of functional Na^+-K^+-ATPase in *Xenopus* oocytes, Am. J. Physiol. 257 (1989) C851–C858.
[34] V. Cattori, J.E. van Montfoort, B. Stieger, L. Landmann, D.K.F. Meijer, K.H. Winterhalter, P.J. Meier, B. Hagenbuch, Localization of organic anion transporting polypeptide 4 (Oatp4) in rat liver and comparison of its substrate specificity with Oatp1, Oatp2 and Oatp3, Pflugers Arch. 433 (2001) 188–195.
[35] M.D. Garrick, H.C. Kuo, F. Vargas, S. Singleton, L. Zhao, J.J. Smith, P. Paradkar, J.A. Roth, L.M. Garrick, Comparison on mammalian cell lines expressing distinct isoforms of divalent metal transporter 1 in a tetracycline-regulated fashion, Biochem. J. 398 (2006) 539–546.
[36] B. Mackenzie, M.L. Ujwal, M.H. Chang, M.F. Romero, M.A. Hediger, Divalent metal-ion transporter DMT1 mediates both H^+-coupled Fe^{2+} transport and uncoupled fluxes, Pflugers Arch. 451 (2006) 544–558.
[37] M. Tabuchi, N. Tanaka, J. Nishida-Kitayama, H. Ohno, F. Kishi, Alternative splicing regulates the subcellular localization of divalent metal transporter 1 isoforms, Mol. Biol. Cell 13 (2002) 4371–4387.
[38] A. Pietrangelo, The ferroportin disease, Blood Cells Mol. Dis. 32 (2004) 131–138.
[39] J. Morrissey, I.R. Baxter, J. Lee, L. Li, B. Lahner, N. Grotz, J. Kaplan, D.E. Salt, M.L. Guerinot, The ferroportin metal efflux proteins function in iron and cobalt homeostasis in *Arabadopsis*, Plant Cell 21 (2009) 3326–3338.
[40] E. Heilig, R. Molina, T. Donaghey, J.D. Brain, M. Wessling-Resnick, Pharmacokinetics of pulmonary manganese absorption: evidence for increased susceptibility to manganese loading in iron-deficient rats, Am. J. Physiol. Lung Cell. Mol. Physiol. 288 (2005) L887–L893.